DNA Amplification in Neutral Liposomes for Safe and Efficient Gene Delivery

Sangmin Lee,[†,‡] Heebeom Koo,[†] Jin Hee Na,[†,‡] Kyung Eun Lee,[§] Seo Young Jeong,[‡] Kuiwon Choi,[†] Sun Hwa Kim,[†] Ick Chan Kwon,[†,⊥,*] and Kwangmeyung Kim[†,*]

[†]Center for Theragnosis, Biomedical Research Institute, Korea, Institute of Science and Technology, 39-1 Hawolgok-dong, Seongbuk-gu, Seoul 136-791, Republic of Korea, [‡]Department of Life and Nanopharmaceutical Science, Kyung Hee University, 1 Hoegi-dong, Dongdaemun-gu, Seoul 130-701, Republic of Korea, [§]Advanced Analysis Center, Korea Institute of Science and Technology, 39-1 Hawolgok-dong, Seongbuk-gu, Seoul 136-791, Republic of Korea, and [⊥]KU-KIST School, Korea University, 1 Anam-dong, Seongbuk-gu, Seoul 136-701, Republic of Korea

ABSTRACT In general, traditional gene carriers contain strong cationic charges to efficiently load anionic genes, but this cationic character also leads to destabilization of plasma membranes and causes severe cytotoxicity. Here, we developed a PCR-based nanofactory as a safe gene delivery system. A few template plasmid DNA can be amplified by PCR inside liposomes about 200 nm in diameter, and the quantity of loaded genes highly increased by more than 8.8-fold. The liposome membrane was composed of neutral lipids free from cationic charges. Consequently, this system is nontoxic, unlike other traditional cationic gene carriers. Intense red fluorescent protein (RFP) expression in CHO-K1 cells showed that the amplified genes could be successfully transfected to cells. Animal experiments with the luciferase gene also showed *in vivo* gene expression by our system without toxicity. We think that this PCR-based nanofactory system can overcome the toxicity problem that is the critical limitation of current gene delivery to clinical application.

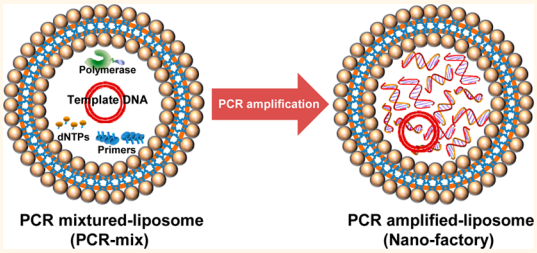

KEYWORDS: polymerase chain reaction · neutral liposomes · gene delivery · nanofactory

Over the last few decades, micro- and nanosized bioreactors consisting of lipid containers have attracted considerable attention as essential tools for understanding the origin of cells in basic life science fields.[1−3] Since liposomes are quite similar in shape and structure to the cellular membrane, liposome-based protocell systems have been extensively studied to perform complex biochemical reaction networks within closed compartments.[4] Recently, several liposome-based models for protocells have been reported to successfully carry out various biochemical reactions, such as genome replication and protein synthesis.[5−11] For instance, Luisi *et al.* first showed that DNA amplification could take place inside the liposomes *via* the polymerase chain reaction (PCR) technique.[12] They established several critical parameters and conditions to stabilize the liposomes at high temperature (95 °C) and increase PCR activity inside the liposomes while maintaining the integrity of DNA products.

The compartmentalization of biochemical reactions is also promising in biomedical applications, including diagnostics and therapeutics. Compared to giant vesicle-based bioreactors (diameter >1 μm), nanosized liposomes in particular may have more opportunities and benefits for the pharmaceutical drug development of bioactive molecules, due to easier access to a single-cell level.[13,14] Since liposome-based nanofactories can locally amplify various bioactive molecules including DNAs, RNAs, and proteins, large amounts of therapeutic products can be loaded into the enveloped vesicles using this technique. The encapsulated biological materials are protected and stabilized *via* the lipid barrier in the extracellular environment. Due to this high stability, liposomes have been extensively studied as promising carrier systems for systemic administration of various therapeutic agents.[15,16]

In this study, we examined the possibility of using a liposome model capable of PCR-induced DNA amplification for gene therapy.

* Address correspondence to K. Kim (kim@kist.re.kr) or I. C. Kwon (ikwon@kist.re.kr).

Received for review October 1, 2013 and accepted April 22, 2014.

Published online April 22, 2014
10.1021/nn501106a

To date, there have been several approaches to the synthesis of oligonucleotides in liposomes, mainly aiming to explore the origin of life. To the best of our knowledge, this is the first report on the use of a PCR-based nanofactory formulated with neutral lipids as a gene delivery system, especially for *in vivo* applications. In general, conventional gene carriers including liposomes contain strong cationic charges to efficiently load anionic genetic drugs, such as plasmid DNA (pDNA), antisense oligodeoxynucleotide (ODN), and small interfering RNA (siRNA).[17] Unfortunately, however, this cationic character also leads to destabilization of plasma membranes and causes severe cytotoxicity.[18] Therefore, gene carriers containing cationic charges basically cannot be set free from the toxicity issue, which is the critical impediment to their clinical application. Herein, we suggest a PCR-based nanofactory using neutral liposomes as a potential gene delivery system to address both efficiency and toxicity issues simultaneously (Scheme 1). PCR-induced DNA amplification inside the liposomes may allow poor DNA loading efficiency of neutral lipid-based liposomes to be overcome.

RESULTS AND DISCUSSION

Preparation and Characterization of PCR-Based Nanofactory. To prepare PCR-based nanofactories, nanosized liposomes encapsulating a pDNA template and PCR components including polymerase, primers, and deoxynucleotides (dNTPs) were made using the film hydration and the freeze− thaw method with subsequent extrusion, immediately followed by 20 PCR cycles (Scheme 1). In our system, the pDNA template and PCR components were loaded into neutral lipid-based liposomes composed of cholesterol, 1,2-dioleoyl-*sn*-glycero-3-phosphoethanolamine (DOPE), and 1,2-dipalmitoyl-*sn*-glycero-3-phosphocholine (DPPC).[19,20] The film composed of the lipid mixture was hydrated and dispersed with PCR solution containing pDNA template, polymerase, primers, and dNTPs. After the formation of large unilamellar vesicles *via* 10 freeze−thaw cycles, the heterogeneous liposomes were passed through cellulose acetate membrane filters with a diameter of 200 nm to yield the desired homogeneous liposome population. To exclude the possibility of undesirable DNA oligomers being amplified outside the liposomes, the pDNA template remaining in the exterior aqueous phase was removed *via* DNase I digestion. In order to visualize exogenous gene expression *in vitro*, red fluorescent protein (DsRed2) was used as a reporter gene inserted into a pDNA template first (Figure 1a). For precise analysis of the linear DNA oligomers, they are retrieved by organic solvents after DNase treatment. After agarose gel electrophoresis, we could observe that the linear DNA oligomers with a size of 1.6 kb were produced from a pDNA template in the liposome (Figure 1b). When we treated these purified

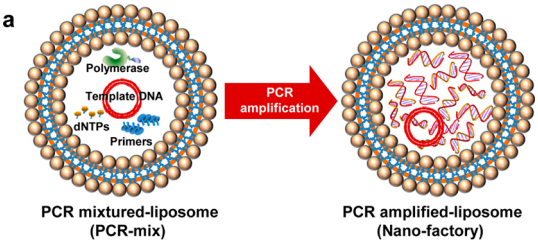

b

Cycle number	Denaturation	Annealing and Elongation
1	2 min at 94°C	
2-21	15 s at 94°C	1.5 min at 68°C

Scheme 1. Development of PCR-based nanofactory system. (a) Schematic illustration of PCR-based nanofactory system. (b) PCR conditions in a liposome.

oligomers with CHO-K1 cells in complex with Lipofectamine 2000 (Lipo2k), they normally expressed red fluorescence originated from DsRed2 (Figure 1c).

After DNA amplification, the PCR-based nanofactory showed liposomes of spherical shape with 204 ± 28.66 nm particle size (Figure 2). There was no significant difference in the size and shape of liposomes before (PCR mix, 174 ± 24.07 nm) and after the PCR amplification (nanofactory). This result strongly indicates that the PCR-based nanofactory could remain stable during the high-temperature PCR phases, consistent with the findings of the previous studies demonstrating that DNA- and RNA-entrapped liposome-based protocell systems could successfully be amplified within a protected microenvironment.[7,12] Although 1,2-dioleoyl-3-trimethylammonium-propane (DOTAP)-based cationic liposomes exhibited a similar particle size (159 ± 35.04 nm), they showed heterogeneous multilamellar structure in parts and thick and dense cationic lipid layers after completion of the PCR process (Supporting Information Figure S1). Originally, the empty nanofactory exhibited a neutral surface charge. Even after encapsulating the pDNA template and conducting the PCR reaction, the resulting nanofactory possessed only a slight negative charge (zeta-potential = −0.62 ± 1.21 mV and −4.24 ± 2.05 mV, respectively). However, the PCR-amplified DOTAP still carried a positive surface charge (58.9 ± 10.9 mV), which was slightly reduced compared to empty DOTAP (69.7 ± 11.5 mV). These results support that the PCR-based nanofactory using a neutral liposome is essentially free from electrostatic interactions between opposite charges, which is the main mechanism of conventional gene carriers.

DNA Amplification inside a Nanofactory. To investigate the production of linear DNA oligomers in the PCR-based nanofactory, the DNA extract solutions from different liposome formulations were analyzed by agarose gel electrophoresis (Figure 3a). On the basis of the pDNA template containing a CMV promotor and the DsRed2 gene sequence, the amplified DNA

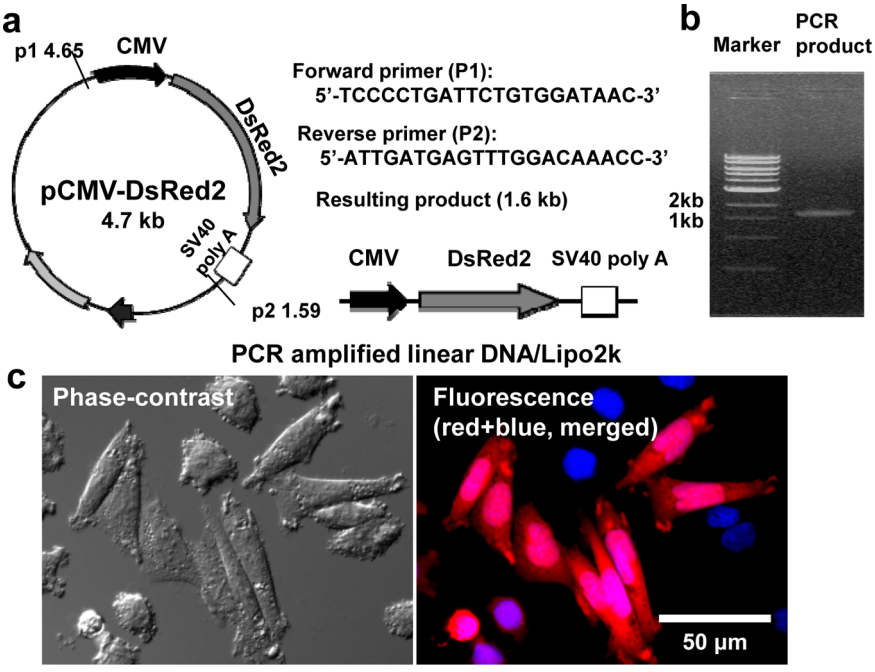

Figure 1. Preparation of PCR-based nanofactory system. (a) Map of pDNA template and designed primers containing the DsRed2 gene (right: linear DNA oligomers produced with a conventional PCR method). (b) Agarose gel image of linear DNA oligomers amplified by PCR. (c) Microscopic images of CHO-K1 cells after transfection using PCR-amplified linear DNA oligomers. The oligomers were complexed with Lipofectamine 2000 (Lipo2k) and incubated with CHO-K1 cells for 6 h. The images were shot after washing and further incubation for 48 h.

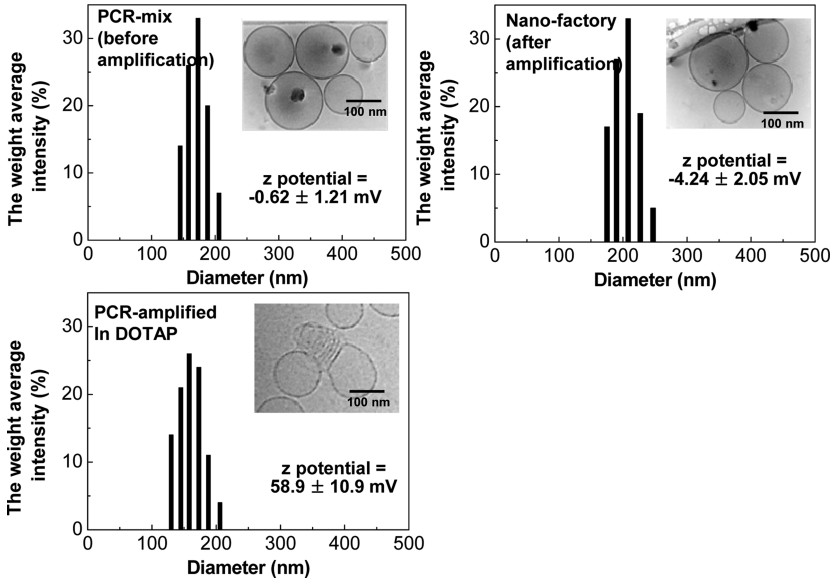

Figure 2. Size distributions of the liposomes encapsulating a PCR mixture (PCR mix), PCR-amplified neutral liposomes (nanofactory), and PCR-amplified DOTAP liposomes measured by DLS. The insets show CryoTEM images.

oligomer is expected to be 1.6 kb in length under general PCR amplification with rationally designed primers. Indeed, the resulting 1.6 kb linear DNA product was obtained *via* the PCR-based nanofactory systems. The DNA products amplified inside the nanofactory still remained even after DNase digestion, while the resultant DNA oligomers in conventional PCR amplification were completely degraded during DNase treatment (Figure 3b). In particular, the nanofactory method could efficiently incorporate DNA products into a neutral liposome formulation. However, when we used a general DNA-loading method for the loading of DNA products post-PCR amplification, it showed poor DNA loading efficiency in neutral liposomes, owing to the absence of charge−charge interactions (Figure 3c, Supporting Information Figure S2). This low DNA loading efficiency is the main reason that neutral liposomes could not be used for gene delivery despite

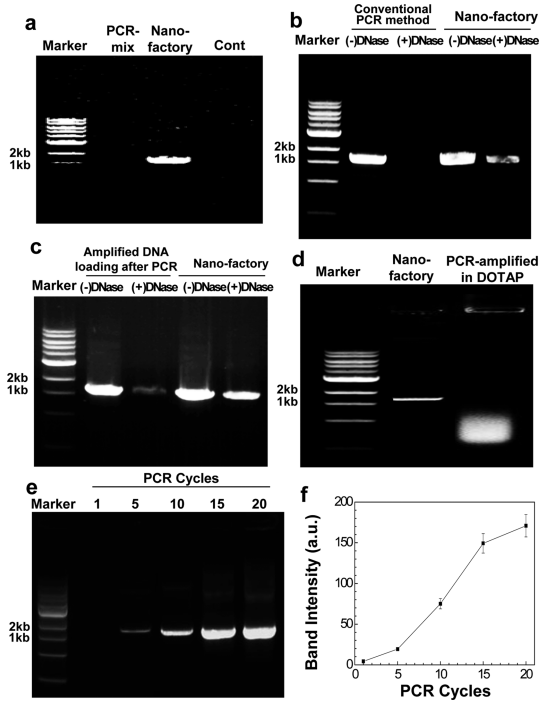

Figure 3. Agarose gel image of PCR-based nanofactory system. (a) Agarose gel image of amplified linear DNA oligomers in a PCR-based nanofactory after 20 PCR cycles. PCR mix: liposomes encapsulating a PCR mixture. Nanofactory: PCR-amplified neutral liposomes. Cont: PCR-amplified liposomes without a pDNA template. (b) Agarose gel image of amplified linear DNA oligomers in a PCR-based nanofactory or conventional PCR method after 20 PCR cycles without liposomes. (c) Encapsulation of DNA products in a PCR-based nanofactory. In the case of amplified DNA loading after PCR, linear DNA oligomers were loaded into neutral liposomes after conventional PCR amplification. After PCR and DNA-encapsulation processes, DNase was treated to remove DNA remaining outside the liposomes. (d) PCR-based DNA amplification in the nanofactory and DOTAP. (e) Agarose gel image of the amplified linear DNA oligomers in a PCR-based nanofactory after 1, 5, 10, 15, and 20 thermal cycles. (f) Intensity of the bands of amplified linear DNA oligomers in (e).

their nontoxic nature.[21] Thus, it was hypothesized that increasing DNA concentration within the liposomes *via* PCR amplification may overcome the low DNA loading capacity of neutral liposomes. Unfortunately, the use of DOTAP for generating the surrounding liposome led to the production of no DNA oligomers (1.6 kb) by PCR amplification, and only a broad single band appeared at lower position (Figure 3d). It was presumed to be the small aggregates of DNA primers, dNTP, and cationic lipids. In the case of DOTAP, the pDNA template and primers were possibly adsorbed onto cationic lipids, which greatly hinders their effective participation in the PCR process. This result revealed that cationic liposomes might not be appropriate to perform PCR amplification.

In addition, we compared the amount of amplified linear DNA oligomers in the PCR-based nanofactory after 1, 5, 10, 15, and 20 thermal cycles (Figure 3e). The template plasmid DNA and the linear oligomers after one cycle could not be observed clearly because their amounts were too small. This gel image significantly showed that the amount of amplified linear DNA oligomers increased after multiple PCR cycles. After comparing the intensity of the bands of the linear DNA oligomers, we observed that the nanofactory has about 8.8-fold increased DNA oligomers after 20 PCR cycles compared to the case after 5 cycles (Figure 3f). Therefore, it demonstrates that the amount of genes in the nanofactory was amplified more than 8.8-fold after the PCR cycles because the amount of the template plasmid DNA in the nanofactory before PCR cycles was smaller than the amount of linear DNA oligomers after 5 cycles based on the band intensities.

The amplification of DNA oligomers in the nanofactory was further examined by measuring the fluorescent signals emitted by forming DNA-intercalating dye/DNA complexes.[7] To visualize the production of DNA oligomers in the nanofactory, SYBR Green I dye was included in a PCR solution, and the liposomal membrane was stained with the lipophilic fluorescent dye rhodamine B (Figure 4a). There was a negligible green fluorescence signal in the case of the PCR mix, showing the amount of DNA is low. However, the nanofactory solution in a 96-well plate exhibited intense green fluorescence after conducting PCR, indicating an effective PCR-based DNA amplification (Figure 4b). In particular, we could observe the liposomes of the PCR mix and nanofactory at the single-particle level with super-resolution structured illumination microscopy, where their diameters were around 200 nm (Figure 4c). The green fluorescence signals were detected mainly inside the spherical shape of the liposome, directly showing that DNA oligomers were successfully amplified within our nanofactory.

***In Vitro* Gene Transfection by the Nanofactory and Cell Viability Test.** To test the efficiency of the nanofactory for *in vitro* gene delivery, first its cellular uptake was monitored in CHO-K1 cells by confocal microscopy using the fluorescent-labeled nanofactory.[22] As shown in Figure 5, distinct green (DNA primers) and red dots (liposomes) were found in the cytoplasm within 2 h, indicating successful internalization of nanofactory in the cytosol within 2 h. For precise analysis of their localization, we also treated the cells with endosome-specific fluorescent marker, Endosome tracker-GFP. After 2 h, nanofactories with red fluorescence were predominantly co-localized with endosomes, which is indicative of their endocytosis. According to the transfection data below, they should escape from the endosomes for transcription after a longer time. However, the mechanisms of the cellular uptake and endosome escape of nanofactories are still unknown, and related studies are now ongoing. The absolute amount of internalized neutral liposomes (nanofactory) was

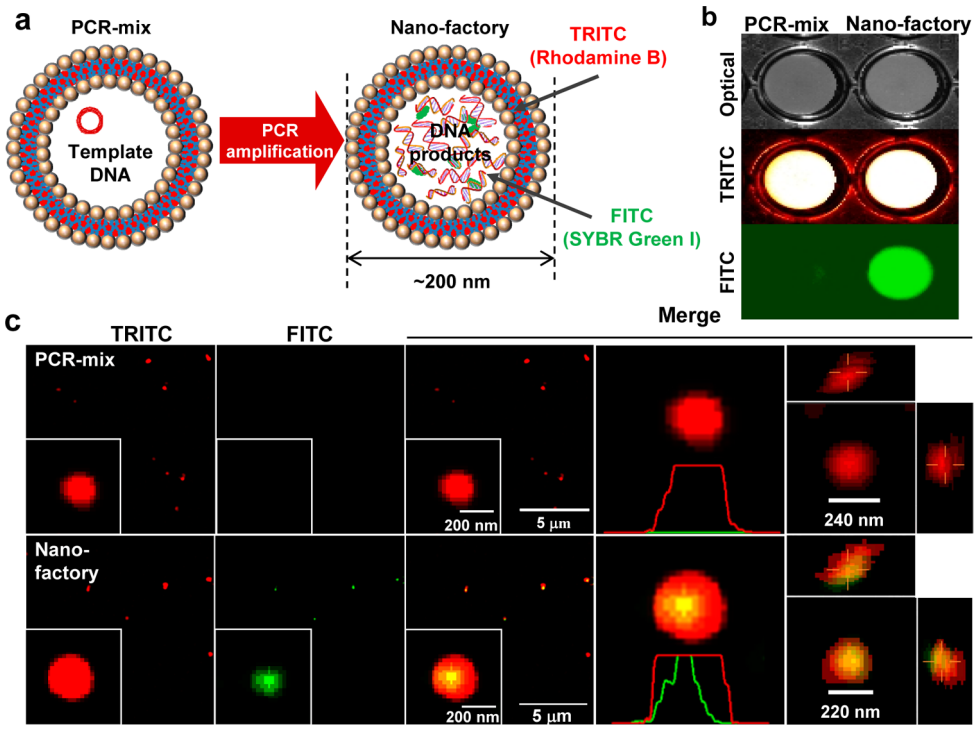

Figure 4. Visualization of DNA amplification in a PCR-based nanofactory system. (a) Schematic illustration of fluorescence signal amplification in the nanofactory through intercalation of SYBR Green dye (FITC filter) into the amplified DNA products. Lipid membrane was stained with rhodamine B (TRITC filter). (b) Fluorescence images of liposomes containing the full PCR components before (PCR mix) and after 20 PCR cycles (nanofactory) in aqueous solutions in a 96-well plate. (c) Confocal microscopic images of the PCR mix and nanofactory. Obtained by super-resolution microscopy (N-SIM).

slightly lower than that of amplified DNA-loaded DOTAP.

In vitro gene transfection efficiency of the PCR-based nanofactory was also evaluated in CHO-K1 cells using a pDNA template containing the DsRed2 gene. The PCR mix showed a very weak red fluorescent signal, which resulted from the entrapped pDNA template, showing the initial amount of genes was obviously insufficient for efficient transfection. After PCRamplification, however, the nanofactory-transfected cells exhibited vivid red fluorescence, indicating that the enhancement of transfection efficiency originated from the amplified linear DNA oligomers, not by the pDNA template (Figure 6a). Interestingly, it achieved a high level of transfection efficiency similar to those of traditional transfection reagents such as BPEI (polyethylenimine, MW 25 kDa) and Lipo2K. The relative fluorescence intensity values of the PCR mixture, nanofactory, BPEI, and Lipo2K were 58.38 ± 15.29, 726.2 ± 51.36, 1127.00 ± 25.72, and 957.23 ± 87.36, respectively (Figure 6b). In spite of the larger amount of DNA after PCR amplification, the transfection efficiency of our nanofactory could not outperform those of traditional cationic carriers. It may originate from the lower cellular uptake due to the absence of the charge−charge interaction between cationic carriers and the cell membrane. However, we think that the cellular uptake can be further enhanced by surface modification of neutral liposomes with various active targeting moieties such as antibodies, aptamers, and peptides. Although cationic reagents seem to have potential as gene carriers with high transfection efficiency, the toxicity issue inevitably limits their use in clinical applications. To show this, the cellular toxicity was assessed by MTT assay before and after PCR amplification and compared to those of conventional cationic gene carriers, BPEI and Lipo2K. As expected, conventional transfection reagents BPEI and Lipo2K exhibited severe cytotoxicity against CHO-K1 cells with IC_{50} values of 8.64 and 12.72 μg/mL, respectively (Figure 6c), mainly owing to their strong cationic charges.[23] On the other hand, neutral lipid-based liposomes with and without PCR amplification showed negligible cytotoxicity even at extremely high carrier concentrations (≥200 μg/mL).

Then, we precisely compared the cytotoxicity, cellular uptake, and transfection efficiency of our nanofactory to amplified DNA-loaded DOTAP. With the same amount of PCR component containing template DNA, we varied the amount of carriers in both nanofactory and amplified DNA-loaded DOTAP. First, the cell viability and mean fluorescence intensity of Cy5-labeled DNA primers of each formulation were analyzed in the same graphs. As expected, more than 90% of cells were alive at 200 μg/mL viability of nanofactory, but the viability decreased to below half with the same concentration of the amplified

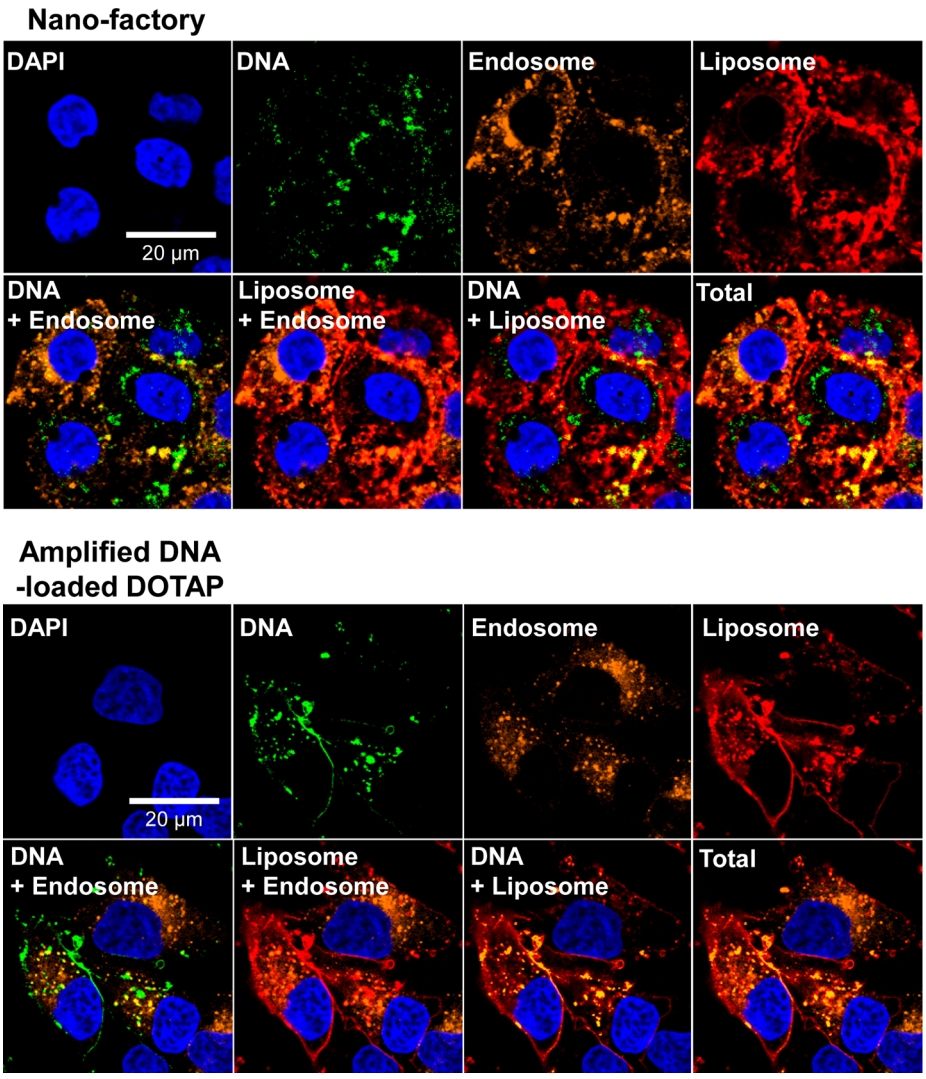

Figure 5. Cellular uptake of nanofactory and amplified DNA-loaded DOTAP in CHO-K1 cells. Cells were treated with nanofactory labeled with Cy5 (green, Cy5-labeled DNA primers) and rhodamine B (red, DOPE-Rhod in liposome). Cells were stained by Endosome tracker-GFP (yellow, endosome) and DAPI (blue, nucleus). Microscopic images were obtained after 2 h. All colors were expressed by pseudocolor mapping.

DNA-loaded DOTAP (Figure 7a and b). At 100 μg/mL carrier condition, cellular uptake of nanofactory was about 58.3% of amplified DNA-loaded DOTAP. This might be due to the absence of the charge−charge interaction between cationic carriers and the cell membrane as mentioned above. In Figure 7c, the transfection efficiency of the nanofactory was enhanced along with the increase of the carrier concentrations. However, the transfection efficiency of amplified DNA-loaded DOTAP started to decrease when the carrier concentration exceeded

20 μg/mL due to their cytotoxicity (Figure 7d). On the basis of these data, we used 200 μg/mL nanofactory and 20 μg/mL DOTAP for the other experiments. The images of CHO-K1 cells treated with these formulations of nanofactory or amplified DNA-loaded DOTAP showed red fluorescence as the result of DsRed2 gene transfection (Figure 7e). This result demonstrates that the PCR-based nanofactory system can result in successful transfection with low toxicity because they have no cationic charges.

Then, we directly compared the transfection efficiencies of two different DNA encapsulation methods, DNA loading before and after PCR amplification. As shown in Figure 3c, the PCR-based nanofactory formulation showed much higher DNA-loading efficiency than the postencapsulation of DNA products obtained after PCR amplification in the aqueous phase. Because of the absence of electrostatic interactions of oppositely charged molecules, the amplified DNA products were not efficiently encapsulated in neutral liposomes and were mainly present outside the liposomes, which resulted in a rapid enzymatic degradation of DNA oligomers. However, the DNA molecules amplified inside the liposomes could remain intact even after DNase attack. As expected from these data, there were big differences in gene transfection efficiency between

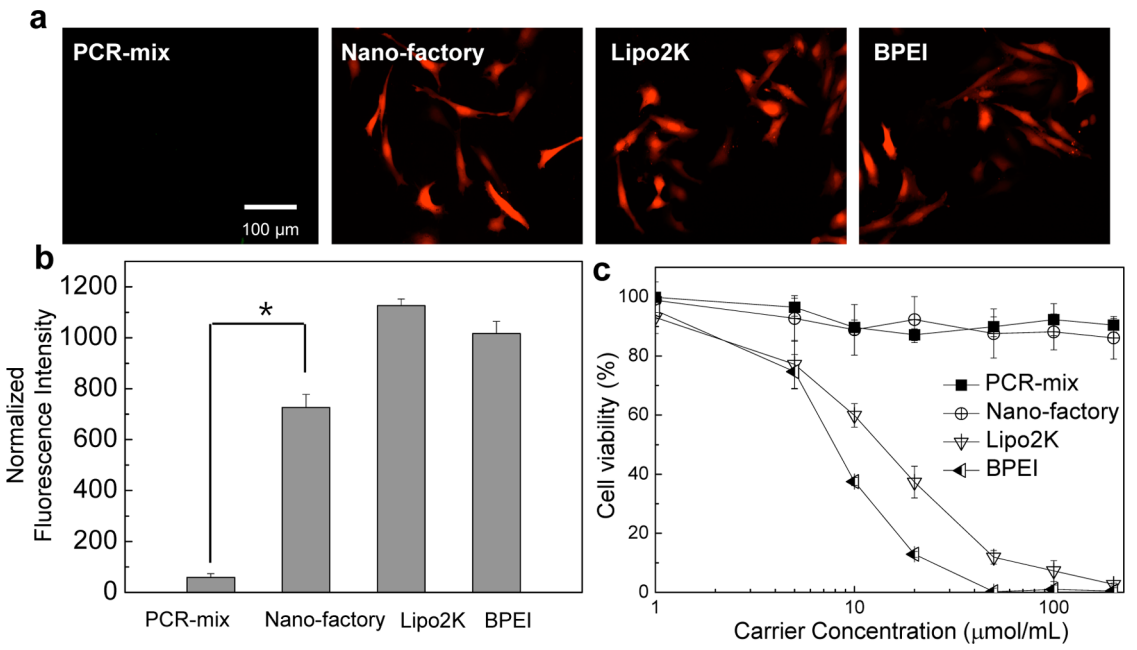

Figure 6. ***In vitro*** **gene transfection efficiency of a PCR-based nanofactory system. (a) Representative fluorescence microscopy images for DsRed2 gene-transfected cells with various DNA formulations. CHO-K1 cells were treated with PCR mix (200 μg/mL, lipid concentration), nanofactory (200 μg/mL, lipid concentration), BPEI (3 μg/mL), and Lipo2k (2 μg/mL). All materials contain 0.5 μg of pDNA, which is the same amount as the pDNA template used in the nanofactory. (b) Mean fluorescence intensities of samples in (a). (c) Cellular toxicity on CHO-K1 cells after transfection with various DNA formulations containing 0.5 μg of pDNA. * shows the difference of the two groups at the $p < 0.05$ significance level.**

these two groups (Supporting Information Figure S3). Even after DNase degradation, the PCR-based nanofactory system exhibited a more than 4-fold increase in fluorescence intensity compared to the postencapsulation of amplified DNA oligomers in neutral liposomes when they are combined with CHO-K1 cells. We think that DNA oligomers were protected by neutral liposomes, and they were released after cellular uptake for transcription.

In Vivo **Gene Transfection by Nanofactory and Histological Analysis.** Finally, we evaluated *in vivo* gene expression with the PCR-based nanofactory system. For *in vivo* studies, we prepared xenograft mice models bearing tumors on both sides of the flank by subcutaneous injection of A549 cells. Then, PCR-based nanofactory containing pGL3-luciferase genes was administered to the right tumor by intratumoral injection once daily for 2 days, while PBS was injected to the left one as a control (Supporting Information Figure S4). After injection of luciferin, the *in vivo* image showed intense luminescence in the right tumor injected with PCR-based nanofactory (Figure 8a). This luminescence signal in the right tumor also could be observed in excised tumors and showed good comparison with the negligible luminescence of the PBS-treated left tumor (Figure 8b). The same experiments with the DsRed2 gene also showed intense red fluorescence in tumor tissue treated with nanofactory (Figure 8c). DOTAP containing amplified DNA oligomers showed more intense luminescence *in vivo*, but histological analysis significantly showed high toxicity (Supporting Information Figure S5). H&E staining showed that there is no difference in tissues treated with PBS and nanofactory, but DOTAP-treated tumor tissue showed significant cell death (Figure 8d). A large number of dark spots in the TUNEL assay demonstrate that apoptosis was brought about by DOTAP. This result showed that the nanofactory can result in a similar level of gene transfection *in vivo* without toxicity compared to cationic gene carriers.

CONCLUSION

In summary, we developed a PCR-based nanofactory as a safe gene delivery system. A few template plasmid DNA can be amplified by PCR inside liposomes, and the quantity of loaded genes significantly increased. The liposome was composed of neutral lipids free from cationic charges. Consequently, this system is nontoxic, unlike other, traditional cationic gene carriers. Intense red fluorescent protein (RFP) expression in CHO-K1 cells showed the amplified genes could be successfully transfected to cells. Animal experiments with the luciferase gene showed *in vivo* gene expression by the nanofactory without toxicity. We think that this PCR-based nanofactory system can overcome the toxicity problem that is the critical impediment of current gene delivery to clinical application. Then, this system will be a useful tool when it is combined with various therapeutic genes such as interleukin-12 for cancer or heme oxygenase-1 for ischemia.[24,25] In addition, surface modification of neutral liposomes with

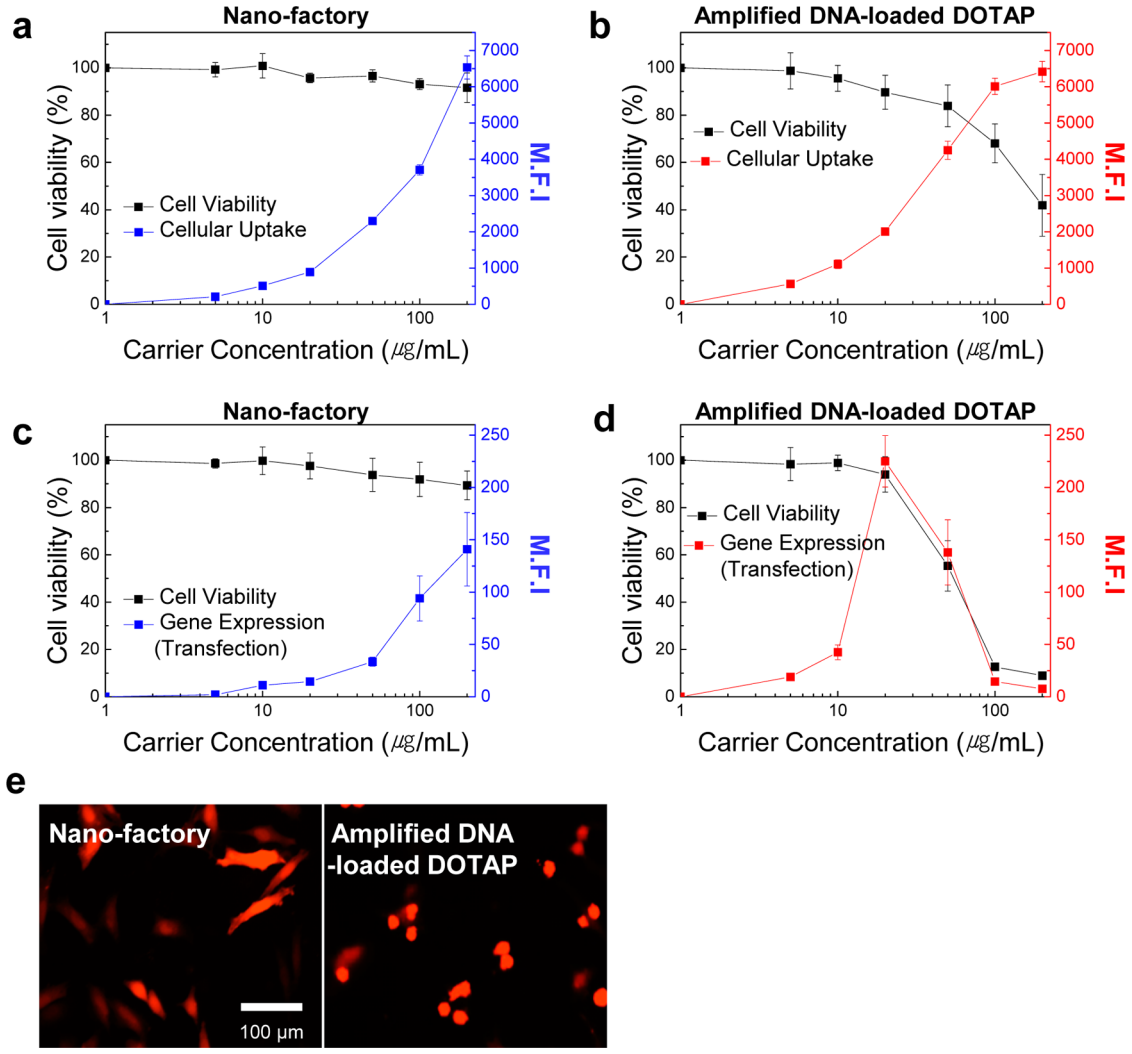

Figure 7. ***In vitro*** **transfection of nanofactory and amplified DNA-loaded DOTAP. Cellular toxicity and cellular uptake of nanofactory (a) and amplified DNA-loaded DOTAP (b) in CHO-K1 cells with varied concentrations of carriers. Cellular toxicity and gene transfection efficiency of nanofactory (c) and amplified DNA-loaded DOTAP (d) in CHO-K1 cells with varied concentrations of carriers. (e) Representative fluorescence microscopy images for DsRed2 gene-transfected cells. CHO-K1 cells treated with nanofactory (200 μg/mL, lipid concentration) and amplified DNA-loaded DOTAP (20 μg/mL, lipid concentration). The same amounts of PCR component containing template DNA were used in all formulations.**

various active targeting moieties such as antibodies, aptamers, and peptides is expected to further increase the cellular uptake and improve the transfection efficiency of the PCR-based nanofactory system.

MATERIALS AND METHODS

Materials. 1,2-Dipalmitoyl-*sn*-glycero-3-phosphocholine (DPPC), 1,2-dioleoyl-*sn*-glycero-3-phosphoethanolamine-*N*-(lissamine rhodamine B sulfonyl) ammonium salt (DOPE-Rhod), cholesterol (CHOL), and 1,2-dioleoyl-3-trimethylammonium-propane (DOTAP) were purchased from Avanti Polar Lipids (Alabaster, AL, USA). The plasmid DNA templates (pCMV-DsRed2 and pGL3-Luciferase) were obtained from Clontech Laboratories (Palo Alto, CA, USA) and Promega (Madison, WI, USA), respectively. DNA primers were purchased from Bioneer (Daejeon, Korea). HiPi Thermostable DNA polymerase and DNase I were bought from ElpisBio (Daejeon, Korea) and Takara (Kyoto, Japan), respectively. SYBR Green I dye and Lipofectamine 2000 were purchased from Invitrogen (Carlsbad, CA, USA). Gel extraction kit and PCR purification kit were purchased from Qiagen (Chatsworth, CA, USA). The Amicon Ultra (3 kDa cutoff) centrifugal filter device was obtained from Millipore (Billerica, MA, USA). Branched polyethylenimine (BPEI) with an average molecular weight of 25 kDa was obtained from Sigma-Aldrich (St. Louis, MO, USA). All other chemicals were of analytical grade and used without further purification. CHO-K1 (Chinese hamster ovary cells) and A549 (human lung adenocarcinoma cells) were purchased from the American Type Culture Collection (Rockville, MD, USA).

PCR Solution. The PCR solution (800 μL) contained deionized water (520 μL), PCR buffer solution (10× HiPi buffer, 100 μL), dNTP mix (2 mM each dNTP in TE buffer, 100 μL), 21-mer primers (10 μM, 20 μL, each), plasmid DNA template (200 ng/μL, 20 μL), and HiPi Thermostable DNA polymerase (1 U μL^{-1}, 20 μL). SYBR Green I dye (0.5×, commercial product diluted 10 000× in TE buffer, 10 μL) was added in the experiments visualizing amplified DNA.

Preparation of Liposomes (PCR-Based Nanofactories). Liposomes were prepared using film hydration and the freeze−thaw

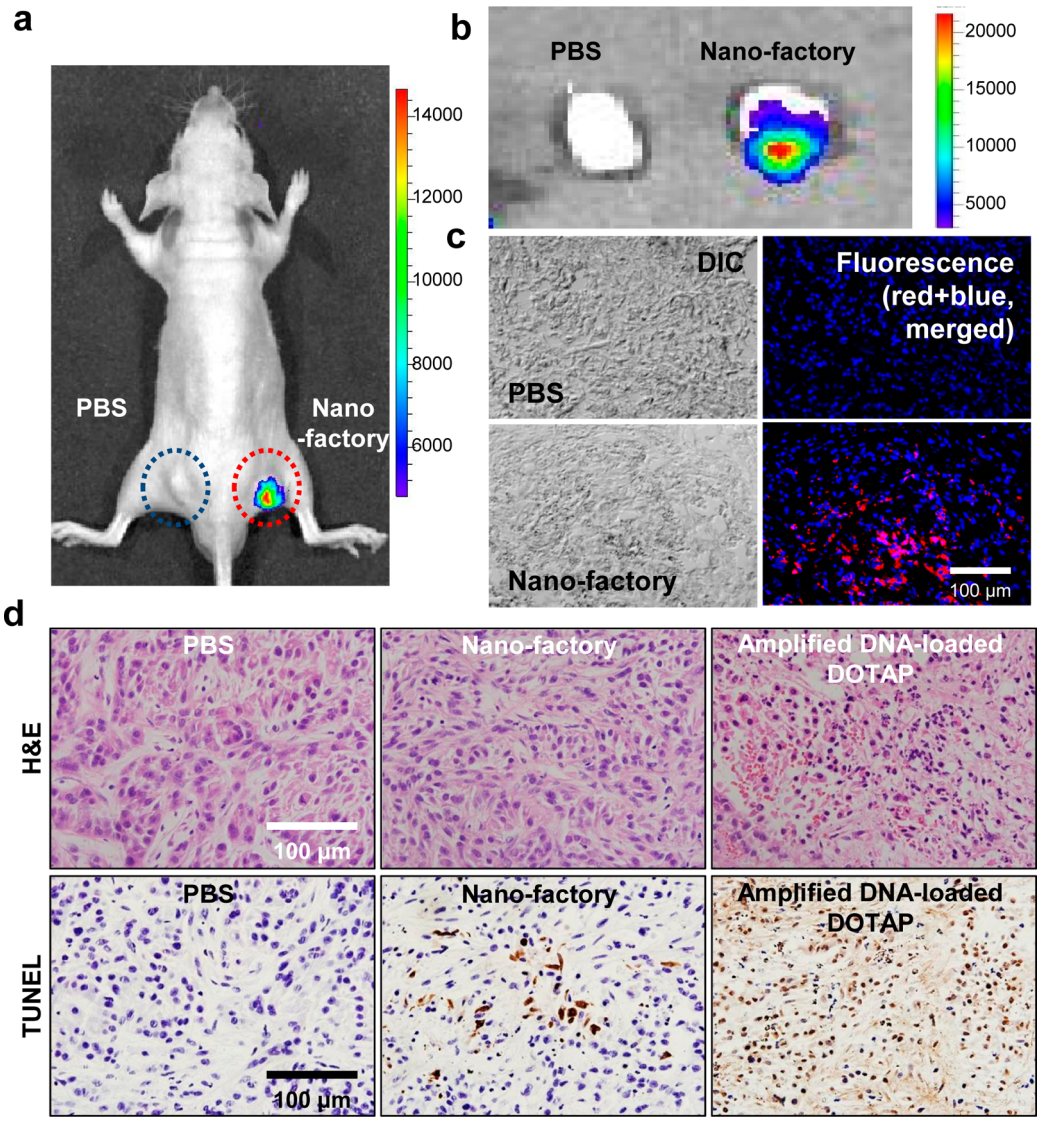

Figure 8. ***In vivo*** **gene expression of PCR-based nanofactory. (a) Bioluminescence imaging of xenograft mice. PBS and nanofactory containing luciferase (10 mg/kg, lipid concentration) were injected intratumorally into tumors on the left and right sides, respectively (once daily for 2 days). Luciferin (50 mg/kg in 200 μL) was injected into the peritoneal cavity 1 day postinjection of nanofactories. At 10 min after luciferin injection, *in vivo* and *ex vivo* images were obtained by IVIS spectrum (exposure time, 60 s). (c) Fluorescence imaging of tumor tissues after intratumoral injection of nanofactory containing the DsRed2 gene. Fluorescence was observed (excitation, 563 nm; emission, 582 nm) using an IX81-ZDC focus drift compensating microscope (exposure time, 500 ms). (d) Histological analysis of tumor tissues treated with PBS, nanofactory (10 mg/kg, lipid concentration), and amplified DNA-loaded DOTAP (1 mg/kg, lipid concentration) by H&E staining (upper) and TUNEL assay (lower).**

method with subsequent extrusion. Dried lipids were mixed in chloroform in a glass vial with the following composition: DPPC:CHOL:DOPE-Rhod = 13:6:1 in molar ratio; total amount of lipid was 2 μmol/sample. The organic solvent was evaporated by rotary evaporator, resulting in the deposition of a thin lipid film on the glass vial wall. The lipid film was freeze-dried overnight to remove traces of remaining organic solvent and then hydrated and dispersed in PCR solution (800 μL) by vortex mixing. Following gentle pipetting, manipulation formed multilamellar vesicles (MLVs) encapsulating the PCR reagents. The MLV dispersion was left for 30 min at room temperature in order to stabilize the morphology of the MLVs. To break the MLVs into large unilamellar vesicles, 10 cycles of freezing with liquid nitrogen and thawing above 50 °C were applied (transition temperature of DPPC is 43 °C.)

The size of liposome was homogenized by extrusion by passing the sample 10-fold through a 200 nm pore cellulose acetate filter. DNase I of 0.002 U/μL in 1× PCR buffer containing 0.5× SYBR Green I dye was added to the liposome dispersion in order to digest the DNA template and primers in the exterior of the liposome (for 5 min, at room temperature). DOTAP liposomes (DOTAP:DOPE = 1:1 molar ratio, total amount of lipid was 2 μmol/sample) were prepared similarly, as mentioned above.

Thermal Cycling. The PCR-based nanofactories were treated with a thermal cycler (Veriti thermal cycler, Applied Biosystems, Foster City, CA, USA) under the following thermal conditions: 94 °C for 2 min [94 °C for 15 s and 68 °C for 1.5 min] × 20 cycles. This condition was applied to the cases of both plasmid DNA templates (pCMV-DsRed2 and pGL3-Luciferase).

Characterization of Liposomes (PCR-Based Nanofactories). The morphology of liposomes was observed by cryogenic transmission electron microscope (cryo-TEM). Each sample was prepared as a thin aqueous film supported on a holey-carbon grid. Cryo-TEM images were obtained at a temperature of approximately −170 °C with a 200 kV Tecnai F20 (FEI, The Netherlands). The average diameter, size distribution, and the surface charge of

liposomes were determined using a Zetasizer Nano ZS (Malvern Instruments, Worcestershire, UK), which is a high-performance two-angle size analyzer using dynamic light scattering and zeta-potential analyzer using electrophoretic light scattering.

Detection of Amplified Linear DNA Oligomers. Amplified linear DNA oligomers of the liposome dispersion were retrieved by the following procedure. A mixture of 150 μL of TE-saturated phenol–chloroform–*iso*-amyl alcohol (25/24/1, v/v/v) was added to nanofactories after DNase I treatment (150 μL), and the enzymes and lipids were removed from the buffered solution containing the amplified linear DNA oligomers. After the aqueous solution was washed with 150 μL of chloroform ($CHCl_3$), the remaining $CHCl_3$ was fully removed by evaporator. Then, the amplified linear DNA oligomers were purified using the PCR purification kit according to the manufacturer's protocol. The purified DNA oligomers were analyzed by agarose gel (1.0%) electrophoresis.

Visualization of DNA Amplification in Liposomes. The PCR-based nanofactories before (PCR mix) and after PCR amplification (nanofactory) were transferred into 96-well plates after DNase I treatment and the amplification of DNA by PCR. Then, they were analyzed by fluorescence with a 12-bit CCD camera (Kodak Image Station 4000 MM, New Haven, CT, USA) equipped with a special C-mount lens and filter set for FITC and TRITC. For more precise observation, the liposome dispersion was mixed with mounting solution (Fluoromount-G, Southern Biotechnology), dropped on a slide, and covered with coverslips. The microscopic images with fluorescence were obtained with super-resolution structured illumination microscopy (SIM, Nikon, Tokyo, Japan).

Cell Culture. CHO-K1 cells were maintained in DMEM (Welgene, Daegu, Korea), supplemented with 10% fetal bovine serum (FBS; Welgene), 100 U/mL penicillin, and 100 μg/mL streptomycin (Welgene) at 37 °C in a humidified 5% CO_2 atmosphere. A549 cells were maintained in RPMI1640 (Welgene), similarly supplemented with 10% FBS, 100 U/mL penicillin, and 100 μg/mL streptomycin.

Gene Expression Test of Amplified Linear DNA Oligomers. The amplified linear DNA oligomers were purified with the gel extraction kit (Qiagen, Chatsworth, CA, USA), and the DNA complexes with Lipofectamine 2000 (Lipo2k) were prepared according to the manufacturer's protocol. CHO-K1 cells were seeded on a 35 mm glass-bottom dish at a density of 5×10^4 cells in 2 mL of serum-free media and grown to reach 60–80% confluence. The culture media were replaced with 2 mL of the transfection medium containing DNA complexes with Lipo2k, followed by a 6 h incubation at 37 °C. The transfection media were then replaced with the fresh complete DMEM media (10% FBS), and the cells were allowed to grow for 48 h. After incubation, the cells were washed twice with Dulbecco's phosphate buffered saline (DPBS) (pH 7.4), fixed with formaldehyde–glutaraldehyde combined fixative for 15 min at room temperature, and then stained with DAPI (Invitrogen, Carlsbad, CA, USA) to label nuclei. All cellular images were obtained using an IX81-ZDC focus drift compensating microscope (Olympus, Tokyo, Japan).

Imaging of Cellular Uptake. In the PCR-based nanofactory system, the buffer was exchanged with DPBS (pH 7.4) using an Amicon Ultra (3 kDa cutoff) centrifugal filter before cell studies and animal experiments. CHO-K1 cells were seeded on a 35 mm glass-bottom dish and allowed to grow until a confluence of 60–80%. One day before the experiment, the cells were incubated with GFP-labeled endosome trackers. Then, they were washed twice with DPBS (pH 7.4) to remove the remnant growth media. The cells were incubated with nanofactories at a lipid concentration of 200 μg/mL for up to 2 h at 37 °C in 2 mL of serum-free media. Then, they were washed twice with DPBS (pH 7.4), fixed with formaldehyde–glutaraldehyde combined fixative for 15 min at room temperature, stained with DAPI (Invitrogen, Carlsbad, CA, USA) to label nuclei, and observed by microscope. To image the location of genes, we used the primers modified with Cy5 fluorescent dye at the 5′ ends for PCR. As a control, amplified DNA-loaded DOTAP with the same amount of labeled DNA primers was used at a lipid concentration of 20 μg/mL.

Cytotoxicity Assay. The cytotoxicity of nanofactories was evaluated by MTT assay. CHO-K1 cells were seeded in 96-well plates at an initial density of 5×10^3 cells per well in 200 μL of the complete media. After 24 h incubation, the media were replaced with 200 μL of fresh complete media, to which PCR mix, nanofactory, BPEI (25 kDa), or Lipo2k was added at varied concentration from 1 to 200 μg/mL. All materials contain 0.5 μg of pDNA, which is the same amount as the pDNA template used in the nanofactory. After additional incubation for 24 h, 25 μL of the (3-(4,5-dimethylthiazol-2-yl)-2,5-diphenyltetrazolium bromide) (MTT) reagent (5 mg/mL in media) was added to each well, and in the absence of light, the cells were incubated for 2 h at 37 °C. Thereafter, 200 μL of DMSO was added to each well. Absorbance at 570 nm was measured with a microplate reader (VERSAmax, Molecular Devices Corp., Sunnyvale, CA, USA).

***In Vitro* Gene Transfection.** For microscopic analysis, DNA complexes with Lipo2k were prepared according to the manufacturer's protocol, and those with BPEI (25 kDa) were prepared at the N/P ratio of 6/1. CHO-K1 cells were seeded on a 35 mm glass-bottom dish at a density of 5×10^4 cells in 2 mL of serum-free media and grown to reach 60–80% confluence. The culture media were replaced with 1 mL of the transfection media containing PCR mix, nanofactory, BPEI, or Lipo2k, followed by 12 h of incubation at 37 °C. All materials contain 0.5 μg of pDNA, which is the same amount as the pDNA template used in the nanofactory. The transfection media were then replaced with the fresh complete DMEM media (10% FBS), and the cells were allowed to grow for 48 h. After incubation, the cells were washed twice with DPBS (pH 7.4), fixed with formaldehyde–glutaraldehyde combined fixative for 15 min at room temperature, and observed by microscope. In a comparative study with amplified DNA-loaded DOTAP, we varied the amount of carriers in both nanofactory and amplified DNA-loaded DOTAP while using the same amount of PCR component containing template DNA.

The quantitative assay was done as follows: The cells were seeded onto a six-well plate at a density of 5×10^5 cells in 2 mL of media and grown to reach 60–80% confluence. The culture media were replaced with 1 mL of the transfection media containing PCR mix, nanofactory, BPEI, or Lipo2k complex (0.5 μg of pDNA template), followed by 12 h of incubation at 37 °C. The transfection media were then replaced with the fresh complete DMEM media (10% FBS), and the cells were allowed to grow for 48 h. They were washed with DPBS (pH 7.4) and lysed with the cell lysis buffer (Sigma-Aldrich, St. Louis, MO, USA). Total soluble protein concentration was determined by bicinchoninic acid (BCA) protein assay (Pierce, IL, USA). Fluorescence intensity of the samples was measured by use of a fluorescence spectrophotometer (Hitachi F-7000, Tokyo, Japan). The resulting intensity was divided by the quantity of proteins determined in the BCA assay for normalization.

***In Vivo* Transfection and Imaging.** All experiments with live animals were performed in compliance with the relevant laws and institutional guidelines of Korea Institute of Science and Technology (KIST), and institutional committees have approved the experiments. A549 tumors were induced in 4-week-old male athymic nude mice (Institute of Medical Science, Tokyo, Japan) on both sides of the flank by subcutaneous injection of 1.0×10^7 cells. Nanofactories containing luciferase as a target gene were administered into the right tumor once daily for 2 days by intratumoral injection (10 mg/kg, lipid concentration), while the same volume of PBS was injected into the left tumor. Luciferin (50 mg/kg in 200 μL), the substrate of luciferase, was injected into the peritoneal cavity 1 day postinjection of nanofactories. At 10–15 min after luciferin injection, *in vivo* and *ex vivo* images were obtained by an IVIS-spectrum system (PerkinElmer, Waltham, MA, USA). As a control, amplified DNA-loaded DOTAP with the same amount of DNA primers was used at a lipid concentration of 1 mg/kg.

Histological Analysis. Nanofactories containing DsRed2 as a target gene were administered into the right tumor of the same tumor-bearing mice model once daily for 2 days by intratumoral injection (10 mg/kg), while the same volume of PBS was injected into the left tumor. Tumors were dissected from mice 1 day postinjection of nanofactories. The dissected tumor tissues were retrieved, fixed in 4% formaldehyde solution for 10 min,

embedded in optimum cutting temperature compound (Sakura, Tokyo, Japan), and frozen by a dry ice bath. Sections were cut on a cryostat (6 μm in thickness), picked up on slides with poly-D-lysine, and dried at 45 °C. Fluorescence was observed using an IX81-ZDC focus drift compensating microscope (Olympus). The sliced tumor tissues (6 μm) were stained with hematoxylin and eosin (H&E) and terminal deoxynucleotidyl transferase UTP nickend labeling (TUNEL) observed with a light microscope (BX51, Olympus). Images were photographed on a digital camera photomicroscope (DP71, Olympus). As a control, amplified DNA-loaded DOTAP with the same amount of DNA primers was used at a lipid concentration of 1 mg/kg.

Statistics. In this paper, the differences between the two groups were analyzed by one-way ANOVA and determined to be statistically significant (marked with an asterisk (*) in figure) if $p < 0.05$.

Conflict of Interest: The authors declare no competing financial interest.

Acknowledgment. This study was funded by the Global Innovative Research Center (GiRC) program and GRL program (NRF-2013K1A1A2A02050115) of the National Research Foundation of Korea and the intramural Research Program (KIST Young Fellow) of KIST.

Supporting Information Available: Additional data are included in supplementary figures. This material is available free of charge *via* the Internet at http://pubs.acs.org.

REFERENCES AND NOTES

1. Szostak, J. W.; Bartel, D. P.; Luisi, P. L. Synthesizing Life. *Nature* **2001**, *409*, 387–390.
2. Mann, S. Systems of Creation: The Emergence of Life from Nonliving Matter. *Acc. Chem. Res.* **2012**, *45*, 2131–2141.
3. Mann, S. The Origins of Life: Old Problems, New Chemistries. *Angew. Chem., Int. Ed.* **2013**, *52*, 155–162.
4. Dzieciol, A. J.; Mann, S. Designs for Life: Protocell Models in the Laboratory. *Chem. Soc. Rev.* **2012**, *41*, 79–85.
5. Mansy, S. S.; Schrum, J. P.; Krishnamurthy, M.; Tobe, S.; Treco, D. A.; Szostak, J. W. Template-Directed Synthesis of a Genetic Polymer in a Model Protocell. *Nature* **2008**, *454*, 122–125.
6. Schroeder, A.; Goldberg, M. S.; Kastrup, C.; Wang, Y.; Jiang, S.; Joseph, B. J.; Levins, C. G.; Kannan, S. T.; Langer, R.; Anderson, D. G. Remotely Activated Protein-Producing Nanoparticles. *Nano Lett.* **2012**, *12*, 2685–2689.
7. Kurihara, K.; Tamura, M.; Shohda, K.-i.; Toyota, T.; Suzuki, K.; Sugawara, T. Self-Reproduction of Supramolecular Giant Vesicles Combined with the Amplification of Encapsulated DNA. *Nat. Chem.* **2011**, *3*, 775–781.
8. Yu, W.; Sato, K.; Wakabayashi, M.; Nakaishi, T.; Ko-Mitamura, E. P.; Shima, Y.; Urabe, I.; Yomo, T. Synthesis of Functional Protein in Liposome. *J. Biosci. Bioeng.* **2001**, *92*, 590–593.
9. Ishikawa, K.; Sato, K.; Shima, Y.; Urabe, I.; Yomo, T. Expression of a Sascading Genetic Network within Liposomes. *FEBS Lett.* **2004**, *576*, 387–390.
10. Noireaux, V.; Libchaber, A. A Vesicle Bioreactor as a Step Toward an Artificial Cell Assembly. *Proc. Natl. Acad. Sci. U.S. A.* **2004**, *101*, 17669–17674.
11. Murtas, G.; Kuruma, Y.; Bianchini, P.; Diaspro, A.; Luisi, P. L. Protein Synthesis in Liposomes with a Minimal Set of Enzymes. *Biochem. Biophys. Res. Commun.* **2007**, *363*, 12–17.
12. Oberholzer, T.; Albrizio, M.; Luisi, P. L. Polymerase Chain Reaction in Liposomes. *Chem. Biol.* **1995**, *2*, 677–682.
13. Cheng, Z.; Al Zaki, A.; Hui, J. Z.; Muzykantov, V. R.; Tsourkas, A. Multifunctional Nanoparticles: Cost Versus Benefit of Adding Targeting and Imaging Capabilities. *Science* **2012**, *338*, 903–910.
14. Koo, H.; Huh, M. S.; Sun, I.-C.; Yuk, S. H.; Choi, K.; Kim, K.; Kwon, I. C. In Vivo Targeted Delivery of Nanoparticles for Theranosis. *Acc. Chem. Res.* **2011**, *44*, 1018–1028.
15. Torchilin, V. P. Recent Advances with Liposomes as Pharmaceutical Carriers. *Nat. Rev. Drug Discovery* **2005**, *4*, 145–160.
16. Koo, H.; Lee, S.; Na, J. H.; Kim, S. H.; Hahn, S. K.; Choi, K.; Kwon, I. C.; Jeong, S. Y.; Kim, K. Bioorthogonal Copper-Free Click Chemistry in Vivo for Tumor-Targeted Delivery of Nanoparticles. *Angew. Chem., Int. Ed.* **2012**, *51*, 11836–11840.
17. Mintzer, M. A.; Simanek, E. E. Nonviral Vectors for Gene Delivery. *Chem. Rev.* **2008**, *109*, 259–302.
18. Hunter, A. C. Molecular Hurdles in Polyfectin Design and Mechanistic Background to Polycation Induced Cytotoxicity. *Adv. Drug Delivery Rev.* **2006**, *58*, 1523–1531.
19. López-Pinto, J. M.; González-Rodríguez, M. L.; Rabasco, A. M. Effect of Cholesterol and Ethanol on Dermal Delivery from DPPC Liposomes. *Int. J. Pharm.* **2005**, *298*, 1–12.
20. Muthu, M. S.; Kulkarni, S. A.; Raju, A.; Feng, S.-S. Theranostic Liposomes of TPGS Coating for Targeted Co-Delivery of Docetaxel and Quantum Dots. *Biomaterials* **2012**, *33*, 3494–3501.
21. Zou, Y.; Zong, G.; Ling, Y. H.; Perez-Soler, R. Development of Cationic Liposome Formulations for Intratracheal Gene Therapy of Early Lung Cancer. *Cancer Gene Ther.* **2000**, *7*, 683–96.
22. Zhang, G.; Gurtu, V.; Kain, S. R. An Enhanced Green Fluorescent Protein Allows Sensitive Detection of Gene Transfer in Mammalian Cells. *Biochem. Biophys. Res. Commun.* **1996**, *227*, 707–711.
23. Koo, H.; Jin, G.-w.; Kang, H.; Lee, Y.; Nam, K.; Zhe Bai, C.; Park, J.-S. Biodegradable Branched Poly(Ethylenimine Sulfide) for Gene Delivery. *Biomaterials* **2010**, *31*, 988–997.
24. Suzuki, R.; Namai, E.; Oda, Y.; Nishiie, N.; Otake, S.; Koshima, R.; Hirata, K.; Taira, Y.; Utoguchi, N.; Negishi, Y.; Nakagawa, S.; Maruyama, K. Cancer Gene Therapy by IL-12 Gene Delivery Using Liposomal Bubbles and Tumoral Ultrasound Exposure. *J. Controlled Release* **2010**, *142*, 245–250.
25. Hyun, H.; Lee, J.; Hwang, D. W.; Kim, S.; Hyun, D. K.; Choi, J. S.; Lee, J.-k.; Lee, M. Combinational Therapy of Ischemic Brain Stroke by Delivery of Heme Oxygenase-1 Gene and Dexamethasone. *Biomaterials* **2011**, *32*, 306–315.